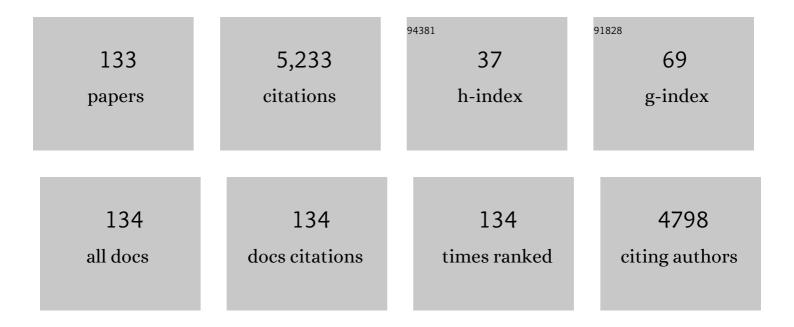
Christoph Arns

List of Publications by Year in descending order

Source: https://exaly.com/author-pdf/8004961/publications.pdf Version: 2024-02-01



#	Article	IF	CITATIONS
1	A Bayesian Optimization Approach to the Simultaneous Extraction of Intrinsic Physical Parameters from <i>T</i> 1 and <i>T</i> 2 Relaxation Responses. SPE Journal, 2023, 28, 319-341.	1.7	1
2	Chemically Induced Evolution of Morphological and Connectivity Characteristics of Pore Space of Complex Carbonate Rock via Digital Core Analysis. Water Resources Research, 2022, 58, .	1.7	6
3	NMR Relaxation Modelling in Porous Media with Dual-Scale-Resolved Internal Magnetic Fields. Transport in Porous Media, 2022, 142, 453-474.	1.2	3
4	A comparison between the characteristics of a biochar-NPK granule and a commercial NPK granule for application in the soil. Science of the Total Environment, 2022, 832, 155021.	3.9	5
5	Lattice Boltzmann framework for accurate NMR simulation in porous media. Physical Review E, 2022, 105, .	0.8	2
6	Digital and experimental rock analysis of proppant injection into naturally fractured coal. Fuel, 2021, 286, 119368.	3.4	16
7	Mechanisms of Confining Pressure Dependence of Resistivity Index for Tight Sandstones by Digital Core Analysis. SPE Journal, 2021, 26, 883-896.	1.7	2
8	Poreâ€5cale MultiResolution Rockâ€Typing of Layered Sandstones via Minkowski Maps. Water Resources Research, 2021, 57, e2020WR029144.	1.7	6
9	Decoupling Minimal Surface Metamaterial Properties Through Multiâ€Material Hyperbolic Tilings. Advanced Functional Materials, 2021, 31, 2101373.	7.8	27
10	Image-based rock typing using local homogeneity filter and Chan-Vese model. Computers and Geosciences, 2021, 150, 104712.	2.0	5
11	Solving Multiphysics, Multiparameter, Multimodal Inverse Problems: An Application to NMR Relaxation in Porous Media. Physical Review Applied, 2021, 15, .	1.5	7
12	Metamaterial Design: Decoupling Minimal Surface Metamaterial Properties Through Multiâ€Material Hyperbolic Tilings (Adv. Funct. Mater. 30/2021). Advanced Functional Materials, 2021, 31, 2170214.	7.8	0
13	A numerical study of field strength and clay morphology impact on NMR transverse relaxation in sandstones. Journal of Petroleum Science and Engineering, 2021, 202, 108521.	2.1	14
14	Highâ€Precision Tracking of Sandstone Deformation From Micro T Images. Journal of Geophysical Research: Solid Earth, 2021, 126, e2021JB022283.	1.4	0
15	A microstructural investigation of a Na2SO4 activated cement-slag blend. Cement and Concrete Research, 2021, 150, 106609.	4.6	25
16	Micro-CT analysis of process-induced defects in composite laminates using AFP. Materials and Manufacturing Processes, 2021, 36, 1561-1570.	2.7	8
17	A solid/fluid substitution scheme constrained by pore-scale numerical simulations. Geophysical Journal International, 2020, 220, 1804-1812.	1.0	3
18	A Poreâ€Scale Upscaling Approach for Laminated Sandstones using Minkowski Maps and Hydraulic Attributes. Water Resources Research, 2020, 56, e2020WR027978.	1.7	7

#	Article	IF	CITATIONS
19	Fast Fourier transform and support-shift techniques for pore-scale microstructure classification using additive morphological measures. Physical Review E, 2020, 101, 033302.	0.8	10
20	Gradient-based fibre detection method on 3D micro-CT tomographic image for defining fibre orientation bias in ultra-high-performance concrete. Cement and Concrete Research, 2020, 129, 105962.	4.6	39
21	A fast FFT method for 3D pore-scale rock-typing of heterogeneous rock samples via Minkowski functionals and hydraulic attributes. E3S Web of Conferences, 2020, 146, 04002.	0.2	1
22	Mechanisms of Confining Pressure Dependence of Resistivity Index for Tight Sandstones. , 2020, , .		0
23	Humidity Effects on Effective Elastic Properties of Rock: An Integrated Experimental and Numerical Study. Journal of Geophysical Research: Solid Earth, 2019, 124, 7771-7791.	1.4	10
24	On the Optimum Aging Time: Magnetic Resonance Study of Asphaltene Adsorption Dynamics in Sandstone Rock. Energy & Fuels, 2019, 33, 8184-8201.	2.5	11
25	A digital rock physics approach to effective and total porosity for complex carbonates: pore-typing and applications to electrical conductivity. E3S Web of Conferences, 2019, 89, 05002.	0.2	4
26	Application of low-field, 1H/13C high-field solution and solid state NMR for characterisation of oil fractions responsible for wettability change in sandstones. Magnetic Resonance Imaging, 2019, 56, 77-85.	1.0	8
27	Porous Media Characterization Using Minkowski Functionals: Theories, Applications and Future Directions. Transport in Porous Media, 2019, 130, 305-335.	1.2	114
28	On the influence of wetting behaviour on relaxation of adsorbed liquids – A combined NMR, EPR and DNP study of aged rocks. Magnetic Resonance Imaging, 2019, 56, 63-69.	1.0	6
29	Relaxation and relaxation exchange NMR to characterise asphaltene adsorption and wettability dynamics in siliceous systems. Fuel, 2018, 220, 692-705.	3.4	31
30	Experimental and Theoretical Evidence for Increased Ganglion Dynamics During Fractional Flow in Mixedâ€Wet Porous Media. Water Resources Research, 2018, 54, 3277-3289.	1.7	50
31	Fast Laplace solver approach to pore-scale permeability. Physical Review E, 2018, 97, 023303.	0.8	22
32	Computation of Relative Permeability From In-Situ Imaged Fluid Distributions at the Pore Scale. SPE Journal, 2018, 23, 737-749.	1.7	23
33	About the connectivity of dual-scale media based on micro-structure based regional analysis of NMR flow propagators. Journal of Contaminant Hydrology, 2018, 212, 143-151.	1.6	5
34	Proceeding of the 13th international Bologna conference on magnetic resonance in porous media (MRPM13). Microporous and Mesoporous Materials, 2018, 269, 1-2.	2.2	0
35	Super resolution reconstruction of <mml:math <br="" xmlns:mml="http://www.w3.org/1998/Math/MathML">id="mml22" display="inline" overflow="scroll" altimg="si1.gif"><mml:mi mathvariant="normal">1¼</mml:mi </mml:math> -CT image of rock sample using neighbour embedding algorithm. Physica A: Statistical Mechanics and Its Applications. 2018. 493. 177-188.	1.2	37
36	The Influence of Syndepositional Macropores on the Hydraulic Integrity of Thick Alluvial Clay Aquitards. Water Resources Research, 2018, 54, 3122-3138.	1.7	8

#	Article	IF	CITATIONS
37	Semi-quantitative multiscale modelling and flow simulation in a nanoscale porous system of shale. Fuel, 2018, 234, 1181-1192.	3.4	19
38	Theoretical investigation of heterogeneous wettability in porous media using NMR. Scientific Reports, 2018, 8, 13450.	1.6	25
39	Three-dimensional porous structure reconstruction based on structural local similarity via sparse representation on micro-computed-tomography images. Physical Review E, 2018, 98, .	0.8	24
40	Porous Structure Reconstruction Using Convolutional Neural Networks. Mathematical Geosciences, 2018, 50, 781-799.	1.4	60
41	Dynamic imaging of multiphase flow through porous media using 4D cumulative reconstruction. Journal of Microscopy, 2018, 272, 12-24.	0.8	2
42	Imaging analysis of fines migration during water flow with salinity alteration. Advances in Water Resources, 2018, 121, 150-161.	1.7	45
43	Regional analysis techniques for integrating experimental and numerical measurements of transport properties of reservoir rocks. Advances in Water Resources, 2017, 100, 48-61.	1.7	6
44	An Experimental and Numerical Study of Relative Permeability Estimates Using Spatially Resolved \$\$T_1\$\$-z NMR. Transport in Porous Media, 2017, 118, 225-250.	1.2	25
45	Pore-Scale Characterization of Two-Phase Flow Using Integral Geometry. Transport in Porous Media, 2017, 118, 99-117.	1.2	73
46	Characterization of reactive flow-induced evolution of carbonate rocks using digital core analysis - part 2: Calculation of the evolution of percolation and transport properties. Journal of Contaminant Hydrology, 2017, 204, 11-27.	1.6	11
47	High-fidelity replication of thermoplastic microneedles with open microfluidic channels. Microsystems and Nanoengineering, 2017, 3, 17034.	3.4	70
48	Numerical Simulation of Reactive Transport on Micro-CT Images. Mathematical Geosciences, 2016, 48, 963-983.	1.4	67
49	Temperature-Dependent Oxygen Effect on NMR D-\$\$T_2\$\$ Relaxation-Diffusion Correlation of n-Alkanes. Applied Magnetic Resonance, 2016, 47, 1391-1408.	0.6	21
50	Investigation of early hydration dynamics and microstructural development in ordinary Portland cement using 1H NMR relaxometry and isothermal calorimetry. Cement and Concrete Research, 2016, 83, 131-139.	4.6	67
51	Experimental and Numerical Investigation on Stress Dependence of Sandstone Electrical Properties and Deviations from Archie's Law. , 2016, , .		6
52	Computation of Relative Permeability from In Situ Imaged Fluid Distributions at the Pore Scale. , 2016, ,		1
53	Characterization of reactive flow-induced evolution of carbonate rocks using digital core analysis- part 1: Assessment of pore-scale mineral dissolution and deposition. Journal of Contaminant Hydrology, 2016, 192, 60-86.	1.6	29
54	Image-based relative permeability upscaling from the pore scale. Advances in Water Resources, 2016, 95, 161-175.	1.7	51

#	Article	IF	CITATIONS
55	An Analysis of Sleeve Effects for Petrophysical Measurements using Digital Core Analysis. , 2015, , .		0
56	Evaluation of Capillary Pressure Methods via Digital Rock Simulations. Transport in Porous Media, 2015, 107, 623-640.	1.2	28
57	Pore scale imaging and modelling of coal properties. APPEA Journal, 2015, 55, 468.	0.4	0
58	Computation of Relative Permeability from Imaged Fluid Distributions at the Pore Scale. Transport in Porous Media, 2014, 104, 91-107.	1.2	27
59	Techniques in helical scanning, dynamic imaging and image segmentation for improved quantitative analysis with X-ray micro-CT. Nuclear Instruments & Methods in Physics Research B, 2014, 324, 49-56.	0.6	121
60	An Assessment of the Influence of Micro-porosity for Effective Permeability Using Local Flux Analysis on Tomographic Images. , 2014, , .		9
61	Percolation Effects of Grain Contacts in Partially Saturated Sandstones: Deviations from Archie's Law. Transport in Porous Media, 2013, 96, 457-467.	1.2	17
62	The heterogeneity in femoral neck structure and strength. Journal of Bone and Mineral Research, 2013, 28, 1022-1028.	3.1	21
63	Micro-Petrophysical Experiments Via Tomography and Simulation. , 2013, , 238-253.		2
64	Correlations Between NMR-Relaxation Response and Relative Permeability From Tomographic Reservoir-Rock Images. SPE Reservoir Evaluation and Engineering, 2013, 16, 369-377.	1.1	10
65	Rock-typing using the complete set of additive morphological descriptors. , 2013, , .		7
66	Permeability Upscaling for Carbonates From the Pore Scale by Use of Multiscale X-Ray-CT Images. SPE Reservoir Evaluation and Engineering, 2013, 16, 353-368.	1.1	38
67	Microtomographic Characterization of Dissolution-Induced Local Porosity Changes Including Fines Migration in Carbonate Rock. SPE Journal, 2013, 18, 545-562.	1.7	42
68	Micro-tomographic Characterization of Dissolution-induced Local Porosity Changes including Fines Migration in Carbonate Rock. , 2012, , .		5
69	Predicting Relative Permeability from NMR Relaxation-Diffusion Responses Utilizing High Resolution Micro Xray-CT Images. , 2012, , .		2
70	Qualitative and Quantitative Analyses of the Three-Phase Distribution of Oil, Water, and Gas in Bentheimer Sandstone by Use of Micro-CT Imaging. SPE Reservoir Evaluation and Engineering, 2012, 15, 706-711.	1.1	48
71	Tuning Elasticity of Openâ€Cell Solid Foams and Bone Scaffolds via Randomized Vertex Connectivity. Advanced Engineering Materials, 2012, 14, 120-124.	1.6	10
72	Tuning Elasticity of Open-Cell Solid Foams and Bone Scaffolds via Randomized Vertex Connectivity. Advanced Engineering Materials, 2012, 14, n/a-n/a.	1.6	0

Christoph Arns

#	Article	IF	CITATIONS
73	Numerical analysis of nuclear magnetic resonance relaxation–diffusion responses of sedimentary rock. New Journal of Physics, 2011, 13, 015004.	1.2	38
74	Minimal surface scaffold designs for tissue engineering. Biomaterials, 2011, 32, 6875-6882.	5.7	417
75	Morphology and Linearâ€Elastic Moduli of Random Network Solids. Advanced Materials, 2011, 23, 2633-2637.	11.1	44
76	Visualization and numerical analysis of adhesive distribution in particleboard using X-ray micro-computed tomography. International Journal of Adhesion and Adhesives, 2010, 30, 754-762.	1.4	42
77	3D structural analysis: sensitivity of Minkowski functionals. Journal of Microscopy, 2010, 240, 181-196.	0.8	32
78	Tomographic image analysis and processing to simulate micro-petrophysical experiments. , 2010, , .		1
79	Fiber Network Elasticity as Function of Crosslinker Density. Biophysical Journal, 2010, 98, 161a.	0.2	0
80	Boolean reconstructions of complex materials: Integral geometric approach. Physical Review E, 2009, 80, 051303.	0.8	27
81	The correlation of pore morphology, interconnectivity and physical properties of 3D ceramic scaffolds with bone ingrowth. Biomaterials, 2009, 30, 1440-1451.	5.7	297
82	3D Imaging and Simulation of Elastic Properties of Porous Materials. Computing in Science and Engineering, 2009, 11, 65-73.	1.2	48
83	Digital rock physics: 3D imaging of core material and correlations to acoustic and flow properties. The Leading Edge, 2009, 28, 28-33.	0.4	119
84	Finite element modelling of the effective elastic properties of partially saturated rocks. Computers and Geosciences, 2008, 34, 647-657.	2.0	27
85	Elastic and flow properties of carbonate core derived from 3D X ray T images. , 2008, , .		2
86	Pore characterization through propagator-resolved transverse relaxation exchange. Physical Review E, 2008, 77, 051203.	0.8	11
87	Propagator Resolved Transverse Relaxation Exchange Spectroscopy. , 2008, , .		0
88	3D Imaging of Reservoir Core at Multiple Scales; Correlations to Petrophysical Properties and Pore Scale Fluid Distributions. , 2008, , .		9
89	X-Ray Micro-Tomography Applications Of Relevance To The Petroleum Industry. AIP Conference Proceedings, 2007, , .	0.3	1
90	Linear elastic properties of granular rocks derived from Xâ€ray T images. , 2007, , .		10

#	Article	IF	CITATIONS
91	Recent Fourier and Laplace perspectives for multidimensional NMR in porous media. Magnetic Resonance Imaging, 2007, 25, 441-444.	1.0	60
92	Developing a virtual materials laboratory. Materials Today, 2007, 10, 44-51.	8.3	160
93	Assessment of bone ingrowth into porous biomaterials using MICRO-CT. Biomaterials, 2007, 28, 2491-2504.	5.7	370
94	3D Pore Scale Characterisation of Carbonate Core: Relating pore types and interconnectivity to petrophysical and multiphase flow properties , 2007, , .		7
95	Elastic and transport properties of cellular solids derived from three-dimensional tomographic images. Proceedings of the Royal Society A: Mathematical, Physical and Engineering Sciences, 2006, 462, 2833-2862.	1.0	48
96	Fluid substitution in porous rocks with aligned cracks: Theory versus numerical modeling. , 2006, , .		0
97	Velocity-porosity relationships, 1: Accurate velocity model for clean consolidated sandstones, GEOPHYSICS, 68, 1822–1834 Geophysics, 2006, 71, Y3-Y3.	1.4	0
98	Experimental Investigation of Drainage Capillary Pressure Computed From Digitized Tomographic Images. , 2006, , .		10
99	Velocity-Porosity Relationships: Predictive velocity model for cemented sands composed of multiple mineral phases Geophysical Prospecting, 2006, 54, 237-237.	1.0	0
100	Structure and properties of clinical coralline implants measured via 3D imaging and analysis. Biomaterials, 2006, 27, 2776-2786.	5.7	66
101	Quantitative properties of complex porous materials calculated from x-ray \hat{l} 4CT images. , 2006, , .		6
102	Pore Scale Characterization of Carbonates Using X-Ray Microtomography. SPE Journal, 2005, 10, 475-484.	1.7	194
103	What is the Characteristic Length Scale for Permeability? Direct Analysis From Microtomographic Data. , 2005, , .		8
104	Mechanical and transport properties of polymeric foams derived from 3D images. Colloids and Surfaces A: Physicochemical and Engineering Aspects, 2005, 263, 284-289.	2.3	34
105	Second-order analysis by variograms for curvature measures of two-phase structures. European Physical Journal B, 2005, 47, 397-409.	0.6	28
106	Velocity-porosity relationships: Predictive velocity model for cemented sands composed of multiple mineral phases. Geophysical Prospecting, 2005, 53, 349-372.	1.0	24
107	Virtual Materials Design: Properties of Cellular Solids Derived from 3D Tomographic Images. Advanced Engineering Materials, 2005, 7, 238-243.	1.6	20
108	Cross-property correlations and permeability estimation in sandstone. Physical Review E, 2005, 72, 046304.	0.8	101

#	Article	IF	CITATIONS
109	Fluids in porous media: a morphometric approach. Journal of Physics Condensed Matter, 2005, 17, S503-S534.	0.7	63
110	An x-ray tomography facility for quantitative prediction of mechanical and transport properties in geological, biological, and synthetic systems. , 2004, , .		15
111	Investigation of microstructural features in regenerating bone using micro computed tomography. Journal of Materials Science: Materials in Medicine, 2004, 15, 529-532.	1.7	22
112	Virtual permeametry on microtomographic images. Journal of Petroleum Science and Engineering, 2004, 45, 41-46.	2.1	170
113	A comparison of pore size distributions derived by NMR and X-ray-CT techniques. Physica A: Statistical Mechanics and Its Applications, 2004, 339, 159-165.	1.2	78
114	Polymeric foam properties derived from 3D images. Physica A: Statistical Mechanics and Its Applications, 2004, 339, 131-136.	1.2	17
115	Three-dimensional imaging of multiphase flow in porous media. Physica A: Statistical Mechanics and Its Applications, 2004, 339, 166-172.	1.2	89
116	Characterisation of irregular spatial structures by parallel sets and integral geometric measures. Colloids and Surfaces A: Physicochemical and Engineering Aspects, 2004, 241, 351-372.	2.3	74
117	Three-dimensional analysis of cortical bone structure using X-ray micro-computed tomography. Physica A: Statistical Mechanics and Its Applications, 2004, 339, 125-130.	1.2	31
118	Digital Core Laboratory: Properties of reservoir core derived from 3D images. , 2004, , .		42
119	Euler-Poincaré Characteristics of Disordered Media: An Application in Effective Medium Theories. Microscopy and Microanalysis, 2004, 10, 714-715.	0.2	1
120	Relative permeability from tomographic images; effect of correlated heterogeneity. Journal of Petroleum Science and Engineering, 2003, 39, 247-259.	2.1	54
121	Velocityâ€porosity relationships, 1: Accurate velocity model for clean consolidated sandstones. Geophysics, 2003, 68, 1822-1834.	1.4	32
122	Virtual core laboratory: Properties of reservoir rock derived from Xâ€ray CT images. , 2003, , .		4
123	Reconstructing Complex Materials via Effective Grain Shapes. Physical Review Letters, 2003, 91, 215506.	2.9	69
124	PETROPHYSICAL PROPERTIES DERIVED FROM X-RAY CT IMAGES. APPEA Journal, 2003, 43, 577.	0.4	15
125	Micro T facility for imaging reservoir rocks at pore scales. , 2003, , .		8
126	Computation of linear elastic properties from microtomographic images: Methodology and agreement between theory and experiment. Geophysics, 2002, 67, 1396-1405.	1.4	341

#	Article	IF	CITATIONS
127	AccurateVp:Vsrelationship for dry consolidated sandstones. Geophysical Research Letters, 2002, 29, 44-1-44-4.	1.5	12
128	Characterising the Morphology of Disordered Materials. Lecture Notes in Physics, 2002, , 37-74.	0.3	31
129	Euler-Poincaré characteristics of classes of disordered media. Physical Review E, 2001, 63, 031112.	0.8	82
130	Accurate estimation of transport properties from microtomographic images. Geophysical Research Letters, 2001, 28, 3361-3364.	1.5	182
131	Permeability evaluation in a glauconiteâ€rich formation in the Carnarvon Basin, Western Australia. Geophysics, 2000, 65, 46-53.	1.4	11
132	Morphology, Cocontinuity, and Conductive Properties of Anisotropic Polymer Blends. Macromolecules, 1999, 32, 5964-5966.	2.2	17
133	Experimental Verification of Effect of Size on Drainage Capillary Pressure Computed from Digitized Tomographic Images. International Journal of Engineering Research in Africa, 0, 1, 1-10.	0.7	4